Cations Mediate Interactions between the Nicotinic Acetylcholine Receptor and Anionic Lipids

Raymond M. Sturgeon and John E. Baenziger*
Department of Biochemistry, Microbiology, and Immunology, University of Ottawa, Ottawa, Ontario, Canada

ABSTRACT Interactions between the nicotinic acetylcholine receptor (nAChR) and phosphatidic acid (PA) are bidirectional in that membranes containing PA are effective at stabilizing an agonist-responsive nAChR, whereas incorporation of the nAChR into the same membranes leads to a substantial increase in lipid lateral packing density. A previous study suggested that the ability of PA to adopt a dianionic ionization state is key. We monitored the ionization state of PA in both reconstituted and protein-free membranes. In model membranes composed of PA and 3:2 (mol/mol) phosphatidylcholine (PC)/PA, the monoanionic-to-dianionic transition of PA was detected with a pKa of 8.7 and 6.5, respectively. In the reconstituted 3:2 PC/PA membranes, however, PA was stabilized in a monoanionic state at pH values up to 10. Although dianionic PA does not play a role in nAChR function, we found that both the stabilization of monoanionic PA and the concentration of other cations at the bilayer surface can account for changes in bilayer physical properties that are observed upon incorporation of the nAChR into 3:2 PC/PA membranes. A nAChR-induced concentration of cations at the bilayer surface likely mediates interactions between the nAChR and the anionic lipids in its membrane environment.

INTRODUCTION

The earliest attempts to isolate and structurally identify both the agonist-binding and ion channel functions of the nicotinic acetylcholine receptor (nAChR) from *Torpedo* showed that this pentameric ligand-gated ion channel exhibits essential interactions with its membrane environment (1–3). Although the sensitivity of nAChR function to lipid composition is not an unusual characteristic for a membrane protein, the nAChR also exhibits the intriguing ability to modify the physical properties of its surrounding membrane environment in a lipid-selective manner (4–7). Incorporation of the nAChR into a PC membrane containing anionic lipids, particularly phosphatidic acid (PA), leads to a substantial lateral tightening of the bilayer. In contrast, the effects of the nAChR on the physical properties of a PC membrane lacking anionic lipids are minimal (4,5).

The ability of the nAChR to undergo allosteric transitions, and thus flux cations across the membrane, is optimal in a reconstituted PC membrane containing both cholesterol (Chol) and the anionic lipid PA (2–5,8–12). The nAChR in 3:1:1 (mol/mol/mol) PC/PA/Chol membranes (PC/PA/Chol-nAChR) is stabilized predominantly in an agonist-responsive resting conformation similar to the conformation adopted in native membranes (13). In contrast, the nAChR in PC membranes that lack PA and Chol (PC-nAChR) is unresponsive to agonist, because it adopts an ''uncoupled'' conformation, where allosteric communication between the agonist-binding sites and the transmembrane pore is lost, even though these sites adopt structures with pharmacologies suggestive of the resting state (13). One possible mechanism by which membranes influence coupling is by modulating the associations between the ''post-M4'' transmembrane helix and the coupling interface between the agonist-binding and transmembrane pore domains (13). Lipids, such as Chol, may also bind to interhelical sites, stabilizing the transmembrane domain structure (14–17) and thus its ability to interact with the agonist-binding domain. Although both potential mechanisms are intriguing, the molecular details by which lipids ultimately influence function remain to be defined.

We and others have shown recently that anionic lipids exhibit strikingly different efficacies for stabilizing the agonist-responsive resting state (9,18). For example, high levels of PA in a PC membrane are most effective at stabilizing the resting conformation (4,5,8,13,18). Mixtures of PC and phosphatidylglycerol (PG) are less effective, because they stabilize a larger proportion of desensitized nAChRs. In contrast, PC membranes containing either phosphatidylserine (PS) or phosphatidylinositol (PI) are relatively ineffective at stabilizing a resting conformation, because they favor the uncoupled state (18). From a mechanics perspective, an important question to address is why PA, and to a lesser extent PG, is more effective than other anionic lipids in a PC membrane at stabilizing an agonist-responsive nAChR.

The optimal effects of PA on nAChR function could reflect the small size of its headgroup, which will influence lipid packing, leading to altered bulk membrane physical properties (19,20). The inclusion of PA, and to a lesser extent PG, in a reconstituted PC membrane could alter the membrane physical environment in a manner that favors the resting state. Alternatively, or in addition, PA is unique among anionic lipids in that it adopts both mono- and dianionic ionization states (pKa of ~8.7 in pure PA bilayers) (21–23) (Fig. 1 *A*). It has been suggested that the nAChR stabilizes the dianionic form of PA, which may be essential

Submitted September 24, 2009, and accepted for publication November 17, 2009.

*Correspondence: jebaenz@uottawa.ca

Editor: Lukas K. Tamm.

0006-3495/10/03/0989/10 $2.00

doi: 10.1016/j.bpj.2009.11.030

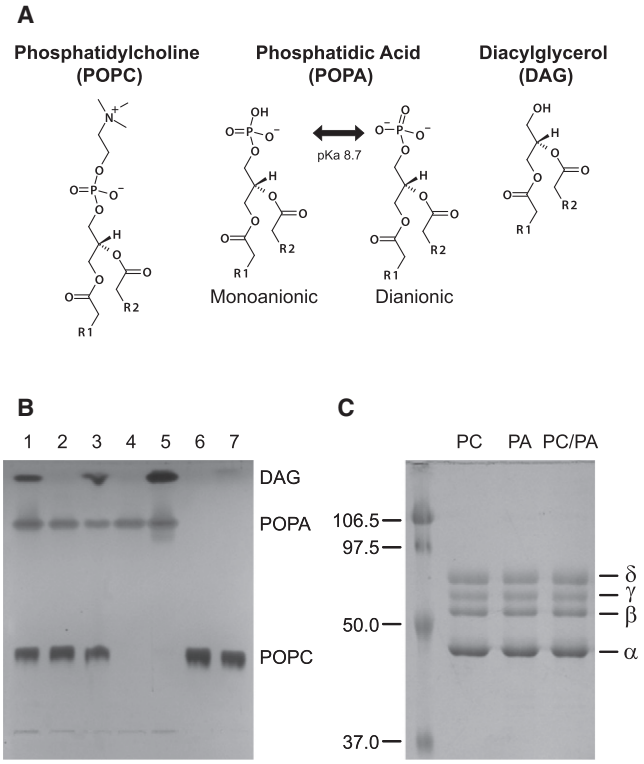

FIGURE 1 Chemical characterization of the reconstituted nAChR membranes. (*A*) Primary lipids used in this study. R refers to the acyl chains: R1, palmitoyl; R2, oleoyl. (*B*) High-performance TLC of lipid standards and lipids extracted from reconstituted nAChR membranes. Lane 1, PC/PA/DAG 3:1.6:0.4 (mol/mol/mol) standard; lane 2, 3:2 (mol/mol) PC/PA standard; lane 3, lipids extracted from 3:2 PC/PA-nAChR; lane 4, PA standard; lane 5, lipids extracted from PA-nAChR; lane 6, PC standard; lane 7, lipids extracted from PC-nAChR. The lipid standards were extracted from aqueous solutions of the cholate-solubilized lipid that were used as lipid washes during affinity purification. (*C*) Sodium dodecyl sulfate polyacrylamide gel electrophoresis of the nAChR from PC-nAChR, PA-nAChR, and PC/PA-nAChR reconstitutions. For each reconstitution, 5 μg nAChR was loaded in the well.

for nAChR function (21). The optimal ability of PA to influence nAChR function could reflect essential interactions between dianionic PA and polar side chains on the nAChR surface.

The initial goals of this study were to test the hypothesis that the nAChR stabilizes the dianionic ionization state of PA and to explore possible mechanisms by which dianionic PA interacts with and thus stabilizes different nAChR conformational states. In contrast to our hypothesis, our data show that the nAChR stabilizes monoanionic PA, likely by concentrating protons at the bilayer surface. Although the ability to form a dianionic ionization state does not play a role in the efficacy of PA at stabilizing the resting nAChR, we find that an nAChR-induced stabilization of monoanionic PA does account for most of the changes in bilayer physical properties that occur upon reconstitution of the nAChR into PA-containing membranes. Our data suggest that the nAChR concentrates cations at the membrane surface in a manner that influences its interactions with surrounding lipids.

MATERIALS AND METHODS

The nAChR was affinity-purified on a bromoacetylcholine affinity column as described elsewhere (4). High-performance thin-layer chromatography (TLC) silica gel plates (60-Å, 4.5-μM, particle size 200 μM) were run using the $CHCl_3/CH_3COH/HCOOH/H_2O$ 50:37.5:3.5:2 (vol/vol/vol/vol) solvent system and stained with Coomassie Blue. Infrared spectra for assessing the pH dependence of lipid phosphate vibrations were recorded using the attenuated total reflectance technique, with nAChR membrane films deposited on a germanium internal reflection element. Protocols for recording the various Fourier transform infrared (FTIR) and fluorescence spectra are described in the Supporting Material.

RESULTS

Characterization of reconstituted nAChR membranes

To test the hypothesis that dianionic PA plays a role in stabilizing a functional nAChR, we first characterized affinity-purified and reconstituted nAChR membranes composed of the lipids PC (PC-nAChR), 3:2 (mol/mol) PC/PA (3:2 PC/PA-nAChR), and PA (PA-nAChR). Sodium dodecyl sulfate polyacrylamide gel electrophoresis shows the expected four-band pattern for each reconstitution, corresponding to the α-, β-, γ-, and δ-subunits at the expected stoichiometric ratio of 2:1:1:1 (Fig. 1 *C*). Each reconstitution also exhibits the expected lipid composition, except that both 3:2 PC/PA-nAChR and PA-nAChR contain an unexpected lipid band whose mobility corresponds to that of diacylglycerol (DAG; Fig. 1 *B*, *lane 1*). Mass spectroscopy confirmed the identity of the unexpected lipid as 1-palmitoyl-2-oleoyl-DAG (42), suggesting that it is a hydrolysis product of the endogenously supplied 1-palmitoyl-2-oleoyl-PA. Based on the lipid standards shown in lane 1 of Fig. 1 *B*, DAG constitutes only ~5 mol % of the final lipid composition of the PC/PA reconstitution, so the actual lipid composition of this membrane is $3:\geq 1.6:\leq 0.4$ (mol/mol/mol) PC/PA/DAG. Control studies suggest that further hydrolysis of PA does not occur after nAChR is reconstituted into the PC/PA membrane (data not shown). For simplicity, we still refer to these membranes as PC/PA-nAChR (see below for further discussion of DAG).

We examined the ability of the nAChR to undergo agonist-induced allosteric transitions in each of the three membranes (Fig. 2). Infrared difference spectra provide a comprehensive map of the vibrational and thus structural changes induced in the nAChR upon agonist binding (24,25). Carbamylcholine (Carb) difference spectra recorded from 3:2 PC/PA-nAChR, PA-nAChR, and PC-nAChR exhibit a positive vibration near 1722 cm^{-1} due to nAChR-bound Carb (26), negative and positive vibrations near 1620 and ~1515 cm^{-1}, respectively, due to physical interactions between the quaternary amine of Carb and aromatic residues,

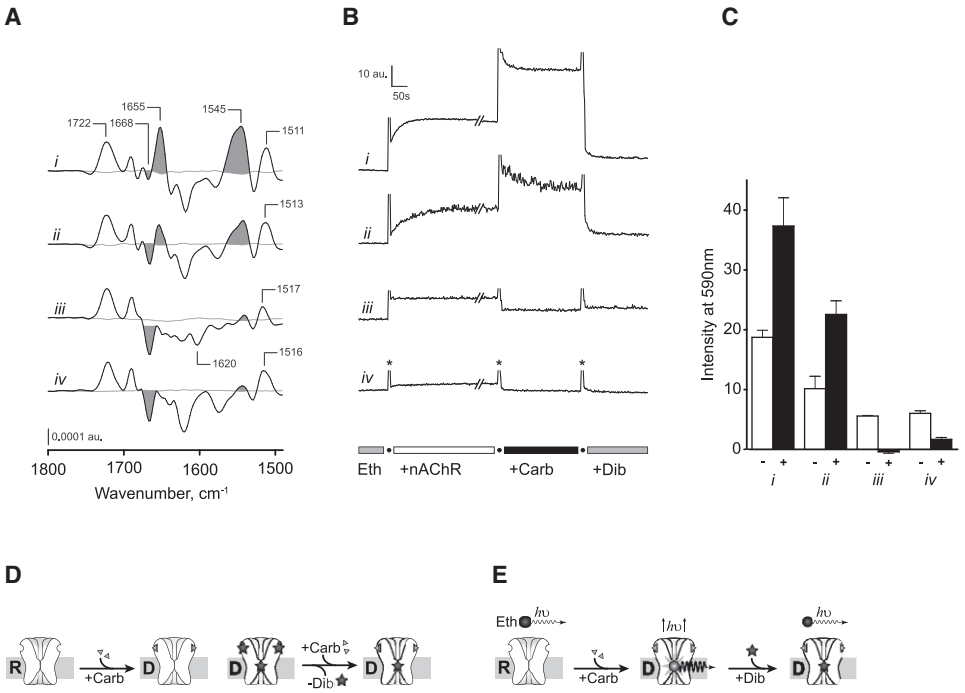

FIGURE 2 Modulation of agonist-induced nAChR conformational change in different membrane environments. (*A*) Carb difference spectra recorded from 3:2 PC/PA-nAChR (*i*), PA-nAChR (*ii*), 3:2 PC/PA-nAChR in the presence of 200 μM dibucaine (*iii*), and PC-nAChR (*iv*). The control spectra, in gray, were obtained from the same samples, but represent the difference between two spectra recorded in the absence of Carb. Spectra shown are averages of at least 55 difference spectra recorded from at least two different reconstitutions. (*B*) Carb-induced changes in ethidium fluorescence for nAChR in the same membranes as in *A*. At the indicated times (*solid circles below spectra*), 30 μg nAChR, 500 μM Carb, and 500 μM dibucaine were added to a 0.3-μM ethidium solution. Asterisks denote breaks where intensity changes due to pipette tip insertion were removed. (*C*) Dibucaine displaceable fluorescence of the nAChR-reconstituted membranes in the absence (−) or presence (+) of 500 μM Carb (mean ± SD, $n = 6$). Labels *i–iv* refer to the traces in *A* and *B*. (*D*) Carb difference spectra are calculated by subtracting a spectrum of the agonist-free state from one of the Carb-bound state. In most cases, these correspond to resting (R) and desensitized (D) states, respectively. The difference spectrum in trace *iii* was held in the D state (with and without Carb) by the presence of excess dibucaine (*stars*). Triangles, Carb. (*E*) Schematic for ethidium fluorescence measurements. Definition of symbols is the same as in *D*.

and a positive vibration near 1690 cm^{-1} due to a physical interaction between the ester of Carb and an unidentified residue in the binding site (27,28). These and other vibrations show that Carb binds to the nAChR in each membrane with a similar pattern of recognition (Fig. 2 *A*).

Carb difference spectra recorded from 3:2 PC/PA-nAChR also exhibit relatively intense positive amide I and II bands near 1655 and 1545 cm^{-1}, respectively, which reflect structural changes induced in the polypeptide backbone upon Carb binding (Fig. 2 *A*, *i*). As these bands are absent from Carb difference spectra recorded from 3:2 PC/PA-nAChR when the reconstituted membrane films are preincubated with the desensitizing local anesthetic dibucaine, we conclude that they reflect the resting-to-desensitized conformational transition (Fig. 2 *A*, *iii*). Comparing the intensities of these two amide vibrations to those observed in Carb difference spectra recorded from native nAChR and PC/PA/Chol-nAChR (data not shown) suggests that a substantial proportion of 3:2 PC/PA-nAChR is stabilized in a resting state that undergoes Carb-induced allosteric transitions. PA-nAChR exhibits moderate positive intensity at both frequencies, suggesting that PA alone can stabilize a resting nAChR (Fig. 2 *A*, *ii*). In contrast, intensity at both frequencies is absent in spectra recorded from PC-nAChR (Fig. 2 *A*, *iv*), because PC-nAChR is ''locked'' in an uncoupled conformation (13).

As a further test of the ability of each membrane to stabilize an agonist-responsive nAChR, we examined the ability of the nAChR in each environment to interact with the conformationally sensitive probe ethidium bromide. Ethidium binds with high affinity to a hydrophobic site within the ion channel pore of the desensitized nAChR ($K_D \cong 0.3$ μM), but not the resting nAChR ($K_D \cong 1$ mM (29). Relative to aqueous ethidium, the nAChR-bound ethidium exhibits greater fluorescence emission intensity, and its emission maximum shifts from 605 (aqueous) to 590 nm (nAChR-bound).

Addition of 3:2 PC/PA-nAChR to 0.3-μM aqueous ethidium leads to an increase in fluorescence emission intensity (Fig. 2 *B*, *i*). Some of this increase is attributable to the scattering of incident light by the membrane vesicles. The remaining slow increase in emission intensity is due to the slow binding of ethidium to sites preexisting in the high-affinity ethidium-binding desensitized state. The addition of 500 μM Carb leads to a substantial increase in dibucaine-displaceable ethidium fluorescence, showing that Carb binding shifts the nAChR pore into a desensitized conformation with high affinity for ethidium. Consistent with the FTIR data, the fluorescence traces show that a proportion of 3:2 PC/PA-nAChR is stabilized in a resting conformation that undergoes Carb-induced allosteric transitions. Also consistent with the FTIR data, a smaller proportion of PA-nAChR is stabilized in an agonist-responsive conformation (Fig. 2 *B*, *ii*). Finally, PC-nAChR adopts an uncoupled conformation that binds ethidium with a low affinity, even in the presence

of Carb (Fig. 2 *B*, *iv*). Collectively, these data show that when included in a reconstituted PC membrane, PA is effective at stabilizing the nAChR in a resting conformation.

Ionization state of PA in model lipid membranes

To determine whether the ability of PA to adopt a dianionic ionization state plays a role in its efficacy at stabilizing a resting nAChR, we first ascertained whether infrared spectroscopy is capable of monitoring PA ionization state in model lipid membranes (i.e., no nAChR) composed of PC, 3:2 PC/PA, and PA. The phosphate stretching region (1250–950 cm^{-1}) in spectra of PC exhibits bands due to both asymmetric ($\nu_a(PO_2^-)$) and symmetric ($\nu_s(PO_2^-)$) stretching of the monoanionic phosphate group near 1230 and 1087 cm^{-1}, respectively (30–32). Other prominent vibrations in this region, near 1067 and 971 cm^{-1}, have been attributed to the ν(C-O-PO_2^-) and $\nu(N^+(CH_3)_3)$ stretching vibrations of the PC headgroup (31–33). The ν(CO-O) vibrations of the two lipid acyl chains also contribute intensity to this region (typically 1150–1180 cm^{-1}). Significantly, these control spectra are virtually superimposable over the entire pH 4–10 range (Fig. 3 *A*, *i*). The lack of spectral changes as a function of pH shows, as expected, that PC does not undergo a change in phosphate headgroup ionization state between pH 4 and 10.

In contrast, control spectra recorded from pure PA membranes exhibit numerous intensity changes over the pH 4–10 range (Fig. 3 *A*, *iii*). Increasing pH converts PA from the mono- to the dianionic ionization state (22,34) and thus leads to a decrease in intensity of vibrations arising from the monoanionic form of PA. The infrared spectra reveal a decrease in intensity of only two bands centered near 1176 and 1070 cm^{-1}. Given that these two vibrations are close in frequency to the vibrational frequencies attributed to the monoanionic phosphate stretching frequencies of PC (see above), nucleotide phosphomonoesters (30,31), and phosphoproteins (30,31) (typically ~1230 and ~1080 cm^{-1}, respectively), we tentatively assign vibrations near 1176 cm^{-1} to the asymmetric ($\nu_a(PO_2^-)$) and those near 1070 cm^{-1} to the symmetric ($\nu_s(PO_2^-)$) stretching vibrations of monoanionic PA. Acyl chain ν(CO-O) and headgroup ν(C-O-PO_2^-) vibrations also contribute substantial intensity to the 1176 and 1070 cm^{-1} vibrations, respectively. Note that an alternative interpretation is that both the symmetric ($\nu_s(PO_2^-)$) stretching vibrations of monoanionic PA and the asymmetric stretching ($\nu_a(PO_3^{2-})$) vibration of dianionic PA (see below) contribute to the band at 1090 cm^{-1}, and that the 1070 cm^{-1} is thus due entirely to the ν(C-O-PO_2^-) vibration of the PA headgroup.

Increasing pH leads to formation of the dianionic form of PA and thus the appearance of new intensity arising from the dianionic stretching of the PA phosphate group. Increasing pH leads to an increase in intensity of two vibrations near 1090 cm^{-1} and 1023 cm^{-1}. Given that these are the only vibrations that increase in intensity with pH, and that their frequencies are similar to the dianionic vibrations of nucleotide phosphomonoesters (30,31) and phosphoproteins (30,31) (1110 and 980 cm^{-1}), we tentatively attribute vibrational intensity near 1090 and 1023 cm^{-1} to the asymmetric ($\nu_a(PO_3^{2-})$) and symmetric ($\nu_s(PO_3^{2-})$) stretching

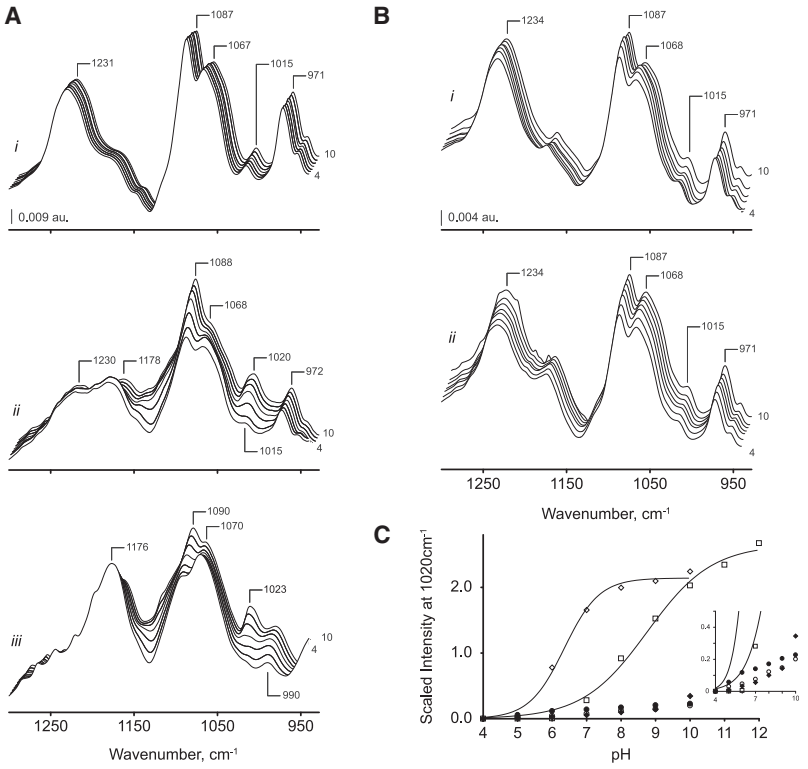

FIGURE 3 The phosphate vibrational region of infrared spectra recorded as a function of pH to monitor the PA ionization state. (*A*) Stacked plots of spectra recorded from pH 4 to pH 10 from (*i*) PC bilayers, (*ii*) 3:2 PC/PA bilayers, and (*iii*) PA bilayers. (*B*) Stacked plots of spectra recorded from pH 4 to pH 10 from (*i*) PC-nAChR and (*ii*) 3:2 PC/PA-nAChR. Spectra in each titration were scaled at the lipid ester carbonyl peak (~1735 cm^{-1}, not shown). Each titration is representative of three different experiments. (*C*) Plot of intensity for the dianionic PA symmetric stretching peak as a function of pH. Boltzmann sigmoidal curves were fitted to the data obtained from the 3:2 PC/PA (*open diamonds*) and PA (*open squares*) bilayers. (*Inset*) Zoomed-in view of the PC and nAChR-reconstituted membranes PC (*open circles*), PC-nAChR (*solid circles*), or 3:2 PC/PA-nAChR (*solid diamonds*).

vibrations, respectively, of dianionic PA. Note that the spectra of PA also exhibit an unassigned band near 990 cm^{-1}, which is close in frequency to the symmetric ($\nu_s(PO_3^{2-})$) dianionic stretching vibrations observed in nucleotide phosphomonoesters and phosphoproteins (30,31). However, this vibration is observed at pH 4, where PA adopts a monoanionic ionization state. It also does not change in intensity with increasing pH and thus cannot be due to the symmetric ($\nu_s(PO_3^{2-})$) stretching vibration of dianionic PA. Further, a plot of the increase in intensity near 1023 cm^{-1} as a function of pH leads to a calculated pKa of 8.7 ± 0.1 for the monoanionic-to-dianionic ionization state transition ($n = 2$) (Fig. 3 *C*, *open squares*), which is identical to values reported in the literature (22,23). The close correlation between the pKa value measured here and those reported in the literature lends support to our infrared band assignments. Of more importance, this correlation shows that regardless of the band assignment, the intensity at 1023 cm^{-1} can be used to monitor the ionization state of PA. An unequivocal assignment of the origin of this vibrational band is beyond the scope of this investigation.

Note also that a precise frequency correlation between the mono- and dianionic phosphate stretching vibrations assigned here for PA and those observed for other biological molecules (i.e., PC, nucleotide phosphomonoesters, and phosphoproteins) is not expected, given the sensitivity of molecular vibrations to local chemistry and environment. Regardless of the band assignments, our control spectra show that pH-dependent changes in intensity at 1176, 1070, 1090, and 1023 cm^{-1} are observed with membranes containing PA. Given the lack of similar intensity changes with pH in control spectra acquired from PC membranes, these pH-dependent changes in intensity can be attributed unequivocally to changes in the PA ionization state, as validated by the pKa measurement.

Finally, the spectra of PC/PA at a 3:2 mol/mol ratio exhibit all the individual features that are observed in spectra of both PC and PA, including the bands tentatively attributed to mono- and dianionic phosphate vibrations, as well as the vibrations due to the choline headgroup of PC, etc. As with the pure PA bilayers, increasing pH leads to increasing intensities of vibrations near 1088 and 1020 cm^{-1} that have been tentatively attributed to dianionic PA. These intensity changes are accompanied by decreasing intensities of vibrations near 1178 and 1068 cm^{-1} that have been attributed tentatively to monoanionic PA. The change in intensity near 1020 cm^{-1} suggests a pKa for the monoanionic-to-dianionic transition of 6.5 ± 0.15 ($n = 3$) (Fig. 3 *C*, *open diamonds*). The drop in pKa in the mixed 3:2 PC/PA versus pure PA membranes likely reflects a combination of effects, including 1), a reduction in electrostatic charge repulsion between adjacent PA molecules when the PA is diluted with PC, and 2), changes in both the physical and chemical environment surrounding the PA headgroup in the PC/PA versus PA bilayers. The latter may lead to novel interactions with divalent cations (20,34). Note that this pKa value is consistent with the membrane phase transition data measured for 3:2 PC/PA membranes at different pH values (see below). Of greatest importance, the above analysis shows that infrared spectroscopy can monitor the ionization state of PA in mixed 3:2 PC/PA bilayers.

Ionization state of PA in reconstituted nAChR membranes

Control spectra were next recorded to test whether infrared spectroscopy can be used to monitor the ionization state of PA in reconstituted nAChR membranes. These controls show that although the nAChR exhibits protein vibrations that overlap with the phosphate vibrations of PC and PA, they are broad and do not distort the main lipid phosphate stretching vibrations (Fig. S1 in the Supporting Material). Also, infrared spectra recorded from PC-nAChR over the pH range of 4–10 (Fig. 3 *B*, *i*) do not reveal changes in the phosphate stretching region that can be attributed to changes in the ionization states of protein side chains. Finally, we recorded spectra of PC-nAChR (and PC/PA-nAChR) over the limited pH 7–10 range. Within experimental error, the spectra are superimposible with the data presented in Fig. 3 (data not shown).

We were surprised to find that infrared spectra recorded from 3:2 PC/PA-nAChR with increasing pH (Fig. 3 *B*, *ii*) exhibit no detectable changes in any of the vibrations in the phosphate stretching frequency region with increasing pH. Specifically, there is no increase in intensity at frequencies attributed to dianionic PA (1088 and 1020 cm^{-1}). There is no decrease in intensity at frequencies attributed to monoanionic PA (1178 and 1068 cm^{-1}). Even at pH 10, the spectra exhibit phosphate vibrational band shapes consistent with the absence of the dianionic form of PA. Specifically, the ratio of the asymmetric dianionic stretching vibration at 1087 cm^{-1} to the symmetric monoanionic stretching frequency near 1067 cm^{-1} in spectra of 3:2 PC/PA-nAChR is similar to the ratio of the same peaks at pH 4 in the spectra of pure 3:2 PC/PA. Also, there is no observed intensity due to the symmetric stretch of dianionic PA near 1020 cm^{-1} in spectra of 3:2 PC/PA-nAChR (note that the weak vibration observed at 1015 cm^{-1} is due to PC (Fig. 3 *A*)). The spectra of 3:2 PC/PA-nAChR show that PA is stabilized in the monoanionic ionization state over the pH range 4–10. This finding is in direct contrast with the suggestion that the nAChR stabilizes the dianionic form of PA (21). We also examined the ionization state of PA in reconstituted PA membranes lacking PC. Although we could not detect any pH-induced changes in the ionization state of PA in these membranes, our data were somewhat inconclusive, because the phosphate stretching vibrational band shapes were distorted relative to those observed in the pure PA bilayers (data not shown). In conclusion, the ability of PA to adopt a dianionic ionization state does not play a role in the efficacy of PA at stabilizing a functional nAChR.

Stabilization of monoanionic PA increases lateral packing density

Although dianionic PA does not play a role in stabilizing a functional nAChR, an nAChR-induced stabilization of mono- over dianionic PA might explain the changes in bilayer physical properties that occur upon incorporation of the nAChR into 3:2 PC/PA membranes. Incorporation of the nAChR into 3:2 PC/PA leads to an increase in the gel-to-liquid-crystal phase transition of the bilayer from ~13 to ~25°C, and a reduction in the degree of water penetration into the bilayer, as monitored by the proportion of lipid ester carbonyls exhibiting strong hydrogen bonds to water (Fig. S2). The changes in both parameters are consistent with a nAChR-induced increase in the lateral packing density of the bilayer. PA in a 3:2 PC/PA membrane lacking the nAChR exists in both mono- and dianionic forms (pKa 6.5, see above). The intermolecular electrostatic repulsion between dianionic PA molecules is greater than that between monoanionic PA molecules (22). A nAChR-induced stabilization of monoanionic PA should thus lead to a reduction in intermolecular lateral charge repulsion and hence might account for the higher lateral packing density observed upon incorporation of the nAChR.

To test whether an nAChR-induced stabilization of monoanionic PA can account for the changes in bilayer physical properties of a 3:2 PC/PA membrane upon incorporation of the nAChR, we compared the physical properties of pure 3:2 PC/PA bilayers (no nAChR) at pH 4, 7, and 10. According to our pKa measurements, these pH values should stabilize monoanionic PA, a mixture of mono- and dianionic PA, and dianionic PA, respectively (Fig. 4 *A*). At pH 10, where the PA headgroup is primarily dianionic, the gel-to-liquid-crystal phase transition of the PC/PA 3:2 bilayers is ~2°C (Table 1). The bilayers at 22.5°C also exhibit a relatively large proportion of strong hydrogen-bonded lipid ester carbonyls, suggesting a relatively high degree of water penetration into the bilayer. The low gel-to-liquid-crystal phase transition and high degree of water penetration both suggest that there is relatively low lateral packing density as a consequence of the high charge repulsion between adjacent molecules of dianionic PA. At pH 7, where there is a mixture of mono- and dianionic PA, the gel-to-liquid-crystal phase transition temperature is ~13°C, which is intermediate between those of PC alone (~4°C) and PA alone (~28°C) (22) at pH 7. In contrast, at pH 4, where PA is predominantly monoanionic, the gel-to-liquid-crystal phase transition of the bilayer increases to ~19°C and there is a much lower degree of water penetration into the bilayer, both effects corresponding to a higher lateral packing density. The ionization state of PA thus has a dramatic effect on the physical properties of a 3:2 PC/PA bilayer. These phase transition temperatures validate our pKa measurements for the PC/PA bilayer. Note, however, that the gel-to-liquid-crystal phase transition temperature of 3:2 PC/PA at pH 4, where PA is monoanionic,

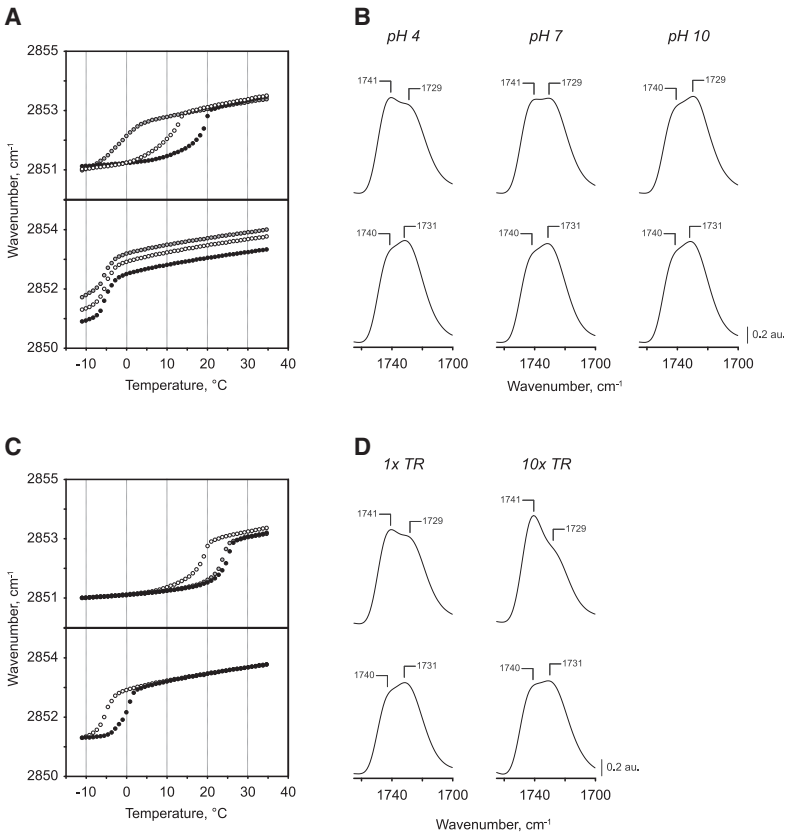

FIGURE 4 Physical properties of lipid bilayers with varying concentrations of cations. (*A*) Temperature dependence of the C-H stretching frequencies observed in spectra of membranes of 3:2 PC/PA (*upper*) and PC (*lower*) at pH 4 (*solid circles*), pH 7 (*open circles*), and pH 10 (*gray circles*). Curves for PC offset for clarity. (*B*) Carbonyl stretching region in deconvolved spectra of lipid bilayers composed of 3:2 PC/PA (*upper*) and PC (*lower*) at pH 4 (*left*), pH 7 (*middle*), and pH 10 (*right*). (*C*) Temperature dependence of the C-H stretching frequencies observed in spectra of 3:2 PC/PA (*upper*) and PC (*lower*) bilayers at pH 4 with 1× (*open circles*), 5× (*gray circles*), and 10× (*black circles*) ions from *Torpedo* Ringer (TR) buffer. (*D*) Carbonyl stretching region in deconvolved spectra of lipid membranes composed of 3:2 PC/PA (*upper*) and PC (*lower*) at pH 4 with 1× (*left*) and 10× (*right*) TR buffer. Spectra in *B* and *D* were deconvolved using GRAMS/AI software with $\gamma = 7$ and smoothing of 75%.

TABLE 1 Effects of the nAChR, pH, salt, and DAG on the gel-to-liquid-crystal phase transition temperatures of PC and PC/PA bilayers

Membrane lipid composition	T_m of pure lipid (°C)	T_m of lipid + nAChR (°C)	Change in T_m with nAChR (°C)	
PC	−3.9 ± 1.8 (4)	−1.8 ± 0.5 (3)	2.1	
PC/PA 3:2	13.1 ± 0.2 (4)	24.7 ± 0.2 (3)	11.6	
	T_m at pH 4 (°C)	T_m at pH 7 (°C)	T_m at pH 10 (°C)	Change in T_m from pH 7 to 4 (°C)
PC	−4.6 ± 0.4 (2)	−3.9 ± 1.8 (4)	−4.4 ± 1.6 (4)	−0.7
PC/PA 3:2	19.0 ± 0.0 (3)	13.1 ± 0.2 (4)	2.3 ± 0.0 (2)	5.9
	T_m 1× TR salt (°C)	T_m 5× TR salt (°C)	T_m 10× TR salt (°C)	Change in T_m from 1× to 10× salt (C°)
PC*	−3.9 ± 1.8 (2)	—	0.7 ± 0.7 (2)	4.6
PC/PA 3:2†	19.0 ± 0.0 (3)	23.6 ± 0.3 (3)	24.8 ± 0.4 (2)	4.8
	T_m of pure lipid (°C)	T_m of lipid + nAChR (°C)	Change in T_m with nAChR (°C)	
PC/PA 3:1	2.9 ± 0.2 (3)	17.7 ± 0.4 (3)	14.8	
PC/DAG 3:1	18.5 ± 0.5 (3)	18.8 ± 1.1 (3)	0.3	
PC/PA/DAG 3:1.5:0.5	17.1 ± 0.4 (3)	—	—	
PC/PA/DAG 3:1:1	20.7 ± 0.2 (3)	25.2 ± 0.4 (3)	4.5	
PC/DAG 3:2	24.1 ± 0.4 (3)	—	—	

Values represent T_m ± SD. Numbers in parentheses represent the number of measurements for each membrane type. *TR*, *Torpedo* Ringer buffer.
*PC bilayers at pH 7.0.
†PC/PA 3:2 bilayers at pH 4.0.

is not as high as that observed for reconstituted 3:2 PC/PA-nAChR. Although the stabilization of monoanionic PA upon incorporation of the nAChR into PC/PA 3:2 membranes may account for some of the observed changes in bilayer physical properties, other phenomena must be involved.

Previous studies have shown that ion channels, including the nAChR and the potassium channel, concentrate cations at the membrane surface (5,35,36). An increased proton concentration could account for the stabilization of monoanionic PA in the presence of the nAChR. We next tested whether an nAChR-induced concentration of the other cations found in *Torpedo* Ringer buffer (Na^+, K^+, Ca^{2+}, and Mg^{2+}) at the bilayer surface might influence bilayer physical properties once PA is already stabilized in the monoanionic state.

The gel-to-liquid-crystal phase transition temperatures and the degree of water penetration into bilayers composed of both pure PC and mixed 3:2 PC/PA membranes were recorded at pH 4.0, where PA is monoanionic, with increasing concentrations of the other cations found in the *Torpedo* Ringer buffer. For both membranes, increasing the concentrations of all cations up to 10 times the initial concentration in *Torpedo* Ringer buffer led to an increase in the gel-to-liquid-crystal phase transition temperature of ~5°C (Fig. 4). The increased cation concentrations also led to a decrease in water penetration into the bilayer. The effects of divalent cations on the phase transitions were slightly more substantial than those of monovalent cations (Table S1). Note that the 3:2 PC/PA membranes at pH 4 with 5 and 10 times the cation concentrations of *Torpedo* Ringer buffer exhibit gel-to-liquid-crystal phase transitions of 24°C and 25°C, respectively, similar to the phase transition temperature of the reconstituted 3:2 PC/PA-nAChR (25°C). In addition, treatment of the 3:2 PC/PA-nAChR membranes with EDTA led to a slight reduction in the gel-to-liquid-crystal phase transition temperature of the bilayer (Table S1). An nAChR-induced increase in local cation concentration at the bilayer surface concomitant with the stabilization of monoanionic PA can thus account for the changes in the physical properties of the 3:2 PC/PA membrane that are observed upon incorporation of the nAChR.

The effects of DAG on bilayer physical properties

Our TLC analysis (Fig. 1 *B*) showed that a small amount of PA is hydrolyzed to DAG during the affinity purification/reconstitution. The appearance of DAG has not been detected previously, possibly due to the fact that previous lipid analyses were not performed using high-performance TLC plates stained with Coomassie Blue. Coomassie Blue has a particular staining efficacy for DAG. Given the small headgroup, it is possible that the presence of DAG might also influence the physical properties of the reconstituted ''PC/PA'' membranes. DAG may thus contribute to the observed changes in bilayer physical properties upon incorporation of the nAChR.

We compared the physical properties of PC/PA membranes containing increasing levels of DAG at the expense of PA. The results presented in the Supporting Material (Fig S3) show that although DAG has a substantial effect on the physical properties of a PC membrane, complete hydrolysis of all the PA in the PC/PA membranes to DAG would be required to achieve a gel-to-liquid-crystal phase transition temperature close to that of 3:2 PC/PA-nAChR. These results suggest that although the formation of DAG contributes to the changes in bilayer physical properties observed upon incorporation of the nAChR, the stabilization of monoanionic PA likely plays a prominent role.

DISCUSSION

PA exhibits an unusual efficacy at stabilizing the nAChR in an agonist-responsive resting state (4,5,8,9,18). The 3:2 PC/PA membrane, which contains small amounts of DAG, is more effective than PC membranes containing PG, PS, PI, or cardiolipin at stabilizing resting versus both desensitized and uncoupled conformations. In fact, the 3:2 PC/PA membrane is as effective as most PC/Chol/anionic lipid mixtures at stabilizing the nAChR in resting conformation that undergoes Carb-induced allosteric transitions. One possible chemical property that could account for the unusual efficacy of PA at stabilizing a resting nAChR is the ability of PA to adopt both mono- and dianionic ionization states. It has been suggested that the nAChR stabilizes dianionic PA, and that interactions between dianionic PA and the nAChR are essential for nAChR function (21). The optimal ability of PA to influence nAChR function could reflect the formation of important interactions between dianionic PA and polar side chains on the surface of the nAChR.

We show here that infrared spectroscopy can monitor the ionization state of PA in both pure PA and mixed 3:2 PC/PA bilayers. We measured the pKa of PA in pure PA and 3:2 PC/PA bilayers as 8.7 and 6.5, respectively, the former being identical to values reported in the literature (22,23). In reconstituted 3:2 PC/PA-nAChR membranes, however, we were unable to detect the transition from mono- to dianionic ionization states with increasing pH. In fact, the phosphate stretching vibrations of the 3:2 PC/PA-nAChR membranes were all indicative of the monoanionic state, even at pH values up to 10. Our data suggest that the nAChR stabilizes the monoanionic, as opposed to the dianionic, form of PA. The unique ability of PA to stabilize a predominantly resting conformation of the nAChR thus cannot be attributed to its unique ability to adopt a dianionic ionization state.

The finding that the nAChR stabilizes the monoanionic form of PA is important in that it shows that PA exhibits the same net ionic charge as other anionic lipids in reconstituted nAChR membrane. As other anionic lipids vary substantially in their ability to stabilize an agonist-responsive nAChR, the ionic charge of PA alone cannot account for its unusual efficacy at stabilizing the nAChR in an agonist-responsive conformation. PA must impart other physical or chemical properties onto a reconstituted PC/PA membrane that are essential for stabilizing a functional state.

One possibility is that PA is more effective than other anionic lipids because of the small size of its headgroup (20,34). A small headgroup will influence the packing of lipids in the bilayer, which in turn will influence the bulk physical properties of the membrane (19). In support of this hypothesis, the anionic lipid PG is also capable of stabilizing a resting nAChR (18). PG, like PA, has a smaller headgroup cross-sectional surface area than other anionic lipids and thus an increased ability to influence the packing of lipids in a PC bilayer (37). The ability of an anionic lipid to influence the bulk physical properties of the membrane may account for the unusual efficacy of PA, and to a lesser extent PG, at stabilizing a functional resting nAChR. Note that the reconstituted PC/PA membranes also contain small amounts of DAG, which could contribute to the efficacy of this bilayer at stabilizing an agonist-responsive receptor. DAG has an even smaller headgroup than PA. The presence of small amounts of DAG in our reconstituted membranes may have a similar impact on bilayer physical properties, contributing to the stabilization of a resting nAChR.

Although the ability of PA to adopt both mono- and dianionic ionization states does not play a role in how PA influences nAChR function, it does play a role in another aspect of nAChR-lipid interactions—the ability of the nAChR to influence the physical properties of its surrounding membrane environment. Incorporation of the nAChR into 3:2 PC/PA membranes leads to a lateral tightening of the bilayer, as shown by an increase in the gel-to-liquid-crystal phase transition temperature and a decrease in the penetration of water into the lipid bilayer. At neutral pH, the PA in a pure 3:2 PC/PA lipid bilayer (i.e., no nAChR) exists in both mono- and dianionic states (pKa = 6.5). Increasing the pH to favor the dianionic form of PA increases the electrostatic repulsion between adjacent PA headgroups, leading to a decrease in the lateral packing density of the bilayer. Conversely, favoring the monoanionic form of PA by decreasing the pH to 4.0 reduces the electrostatic charge repulsion between PA molecules, leading to an increase in lateral packing density. As the incorporation of the nAChR into 3:2 PC/PA bilayers stabilizes monoanionic PA, this should lead to a reduction in the electrostatic charge repulsion between adjacent PA molecules in the reconstituted membrane and thus to a higher lateral packing density. Our quantitative data suggest that an nAChR-induced stabilization of monoanionic PA can account for most of the change in bilayer physical properties observed upon incorporation of the nAChR.

The mechanisms by which the nAChR influence the ionization state of PA are currently unclear. The nAChR could interact directly with adjacent PA molecules to stabilize the monoanionic form. The nAChR has a high affinity for anionic lipids (38,39). Alternatively, the nAChR exhibits a predominantly negative electrostatic surface potential and could thus increase the concentrations of protons at the bilayer surface (Fig. S4). Previous studies have shown that the nAChR does concentrate divalent cations at the bilayer surface (5). Other cation-selective ion channels concentrate protons at the bilayer surface in a manner that enhances ion selectivity (35,36). The nAChR has an overall net negative charge at pH 7 (pI 4.8) and thus would be expected to attract cations in the vicinity of the lipid bilayer.

The remainder of the changes in bilayer physical properties observed upon incorporation of the nAChR into 3:2 PC/PA membranes likely result from an nAChR-induced concentration of other cations at the bilayer surface, as well as from the formation of DAG as a consequence of PA

hydrolysis (42). In model bilayers, increasing the concentration of cations and/or inclusion of DAG both lead to changes in the physical properties of the bilayer that are similar to those observed upon incorporation of the nAChR. Treating 3:2 PC/PA-nAChR membranes with EDTA reverses slightly the effects observed when nAChR is incorporated into the lipid membranes, suggesting a role for divalent cations. Note that incorporation of the nAChR into PC membranes containing other anionic lipids also leads to a lateral tightening of the lipid bilayer, although the effects are not as dramatic as with 3:2 PC/PA membranes (18). An nAChR-induced increase in the local concentration of cations at the membrane surface would account for the moderate changes in bilayer physical properties observed with other PC/anionic lipid mixtures.

Finally, the fact that our reconstituted membranes contain small amounts of the neutral lipid DAG, which likely forms from hydrolysis of PA, is an intriguing finding. We were able to detect this lipid because of a careful TLC analysis, which was initiated because our TLC results consistently showed that the levels of PA were slightly lower than expected in our reconstituted membranes. The TLC plates were washed extensively with solvent immediately before use to eliminate impurities that run at the solvent front and initially obscured the presence of DAG. The detection of DAG in our samples was also a consequence of the use of Coomassie Blue as a lipid staining agent. Coomassie Blue stains DAG with particular intensity. We are currently searching for the catalyst that hydrolyzes PA.

The finding of DAG in our reconstituted membranes and the demonstration that the nAChR influences its membrane microenvironment, possibly by concentrating cations at the bilayer surface, are both of general importance given that molecular dynamics simulations and model membrane studies are increasingly used to understand how specific lipid combinations influence membrane mechanical properties and thus, ultimately, membrane protein function. Our data show that the physical environment created by a specific lipid mixture in a model membrane will not always mimic the physical environment of the same lipids in a reconstituted membrane. Direct measurements of the physical properties of reconstituted nAChR membranes are thus required to draw correlations between membrane mechanical properties and membrane protein function. The effects of DAG and an altered local salt concentration will also have to be taken into account when considering the potential involvement of the nAChR in lipid raft formation (6,7).

In conclusion, our study shows that the ability of PA to adopt a dianionic state does not play a role in its efficacy at stabilizing an agonist-responsive resting nAChR. PA is likely more efficacious than other anionic lipids because it more effectively influences bilayer packing and thus bulk membrane physical properties in a manner that enhances nAChR function. We also show that the nAChR is capable of altering its local membrane environment, likely by concentrating cations at the bilayer surface. It is interesting to note, however, that increasing the cation concentration should generally favor increased deprotonation of PA to the dianionic state, whereas in a reconstituted membrane environment, the nAChR actually stabilizes PA in the monoanionic ionization state. Given that the nAChR is thought to exist within rafts in the plasma membrane, and that its association with lipids plays an important role in both trafficking and membrane localization (40,41), factors that influence how the nAChR interacts with surrounding lipids may have an impact on the localization of the nAChR at a synapse. The possibility that the nAChR concentrates cations at the bilayer surface in a manner that influences how it interacts with its surrounding membrane environment to influence membrane localization obviously requires further investigation.

SUPPORTING MATERIAL

Materials and methods, a table, four figures, and discussion are available at http://www.biophysj.org/biophysj/supplemental/S0006-3495(09)01760-3.

We thank Martin Pelchat for the use of his fluorescence spectrometer, and both Yara Harb and Shuzhi Wang for technical assistance with the preparation of some of the reconstituted membranes.

This work was supported by a Canadian Institutes of Health Research grant to J.E.B.

REFERENCES

1. Heidmann, T., A. Sobel, …, J. P. Changeux. 1980. Reconstitution of a functional acetylcholine receptor. Conservation of the conformational and allosteric transitions and recovery of the permeability response; role of lipids. *Eur. J. Biochem.* 110:35–55.
2. Criado, M., H. Eibl, and F. J. Barrantes. 1984. Functional properties of the acetylcholine receptor incorporated in model lipid membranes. Differential effects of chain length and head group of phospholipids on receptor affinity states and receptor-mediated ion translocation. *J. Biol. Chem.* 259:9188–9198.
3. Fong, T. M., and M. G. McNamee. 1986. Correlation between acetylcholine receptor function and structural properties of membranes. *Biochemistry.* 25:830–840.
4. daCosta, C. J. B., A. A. Ogrel, …, J. E. Baenziger. 2002. Lipid-protein interactions at the nicotinic acetylcholine receptor. A functional coupling between nicotinic receptors and phosphatidic acid-containing lipid bilayers. *J. Biol. Chem.* 277:201–208.
5. daCosta, C. J. B., I. D. Wagg, …, J. E. Baenziger. 2004. Phosphatidic acid and phosphatidylserine have distinct structural and functional interactions with the nicotinic acetylcholine receptor. *J. Biol. Chem.* 279:14967–14974.
6. Poveda, J. A., J. A. Encinar, …, J. M. González-Ros. 2002. Segregation of phosphatidic acid-rich domains in reconstituted acetylcholine receptor membranes. *Biochemistry.* 41:12253–12262.
7. Wenz, J. J., and F. J. Barrantes. 2005. Nicotinic acetylcholine receptor induces lateral segregation of phosphatidic acid and phosphatidylcholine in reconstituted membranes. *Biochemistry.* 44:398–410.
8. Baenziger, J. E., M. L. Morris, …, S. E. Ryan. 2000. Effect of membrane lipid composition on the conformational equilibria of the nicotinic acetylcholine receptor. *J. Biol. Chem.* 275:777–784.
9. Hamouda, A. K., M. Sanghvi, …, M. P. Blanton. 2006. Assessing the lipid requirements of the *Torpedo californica* nicotinic acetylcholine receptor. *Biochemistry.* 45:4327–4337.

10. Ryan, S. E., C. N. Demers, …, J. E. Baenziger. 1996. Structural effects of neutral and anionic lipids on the nicotinic acetylcholine receptor. An infrared difference spectroscopy study. *J. Biol. Chem.* 271: 24590–24597.

11. Sunshine, C., and M. G. McNamee. 1992. Lipid modulation of nicotinic acetylcholine receptor function: the role of neutral and negatively charged lipids. *Biochim. Biophys. Acta.* 1108:240–246.

12. Sunshine, C., and M. G. McNamee. 1994. Lipid modulation of nicotinic acetylcholine receptor function: the role of membrane lipid composition and fluidity. *Biochim. Biophys. Acta.* 1191:59–64.

13. daCosta, C. J. B., and J. E. Baenziger. 2009. A lipid-dependent uncoupled conformation of the acetylcholine receptor. *J. Biol. Chem.* 284:17819–17825.

14. Addona, G. H., H. Sandermann, Jr., …, K. W. Miller. 1998. Where does cholesterol act during activation of the nicotinic acetylcholine receptor? *Biochim. Biophys. Acta.* 1370:299–309.

15. Jones, O. T., and M. G. McNamee. 1988. Annular and nonannular binding sites for cholesterol associated with the nicotinic acetylcholine receptor. *Biochemistry.* 27:2364–2374.

16. Brannigan, G., J. Hénin, …, M. L. Klein. 2008. Embedded cholesterol in the nicotinic acetylcholine receptor. *Proc. Natl. Acad. Sci. USA.* 105:14418–14423.

17. Hamouda, A. K., D. C. Chiara, …, M. P. Blanton. 2006. Cholesterol interacts with transmembrane α-helices M1, M3, and M4 of the *Torpedo* nicotinic acetylcholine receptor: photolabeling studies using [3H]Azicholesterol. *Biochemistry.* 45:976–986.

18. daCosta, C. J. B., S. A. Medaglia, N. Lavigne, S. Wang, C. L. Carswell, and J. E. Baenziger. 2009. Anionic lipids allosterically modulate multiple nicotinic acetylcholine receptor conformational equilibria. *J. Biol. Chem.* 284:33841–33849.

19. Lee, A. G. 2004. How lipids affect the activities of integral membrane proteins. *Biochim. Biophys. Acta.* 1666:62–87.

20. Kooijman, E. E., V. Chupin, …, P. R. Rand. 2005. Spontaneous curvature of phosphatidic acid and lysophosphatidic acid. *Biochemistry.* 44:2097–2102.

21. Bhushan, A., and M. G. McNamee. 1993. Correlation of phospholipid structure with functional effects on the nicotinic acetylcholine receptor. A modulatory role for phosphatidic acid. *Biophys. J.* 64:716–723.

22. Demel, R. A., C. C. Yin, …, H. Hauser. 1992. Monolayer characteristics and thermal behaviour of phosphatidic acids. *Chem. Phys. Lipids.* 60:209–223.

23. Träuble, H., and H. Eibl. 1974. Electrostatic effects on lipid phase transitions: membrane structure and ionic environment. *Proc. Natl. Acad. Sci. USA.* 71:214–219.

24. Baenziger, J. E., S. E. Ryan, and V. C. Kane-Dickson. 2006. Membrane receptor-ligand interactions probed by attenuated total reflectance infrared difference spectroscopy. *In* Vibrational Spectroscopy of Biological and Polymeric Materials. V. G. Gregoriou and M. S. Braiman, editors. Taylor & Francis, Boca Raton, FL. 325–351.

25. Baenziger, J. E., and C. J. B. daCosta. 2008. Membrane protein structure and conformational change probed using Fourier transform infrared spectroscopy. *In* Biophysical Analysis of Membrane Proteins. E. Pebay-Peyroula, editor. Wiley-VCH, Weinheim, Germany. 259–288.

26. Baenziger, J. E., K. W. Miller, and K. J. Rothschild. 1993. Fourier transform infrared difference spectroscopy of the nicotinic acetylcholine receptor: evidence for specific protein structural changes upon desensitization. *Biochemistry.* 32:5448–5454.

27. Baenziger, J. E., S. E. Ryan, …, C. J. daCosta. 2008. Lipid composition alters drug action at the nicotinic acetylcholine receptor. *Mol. Pharmacol.* 73:880–890.

28. Ryan, S. E., D. G. Hill, and J. E. Baenziger. 2002. Dissecting the chemistry of nicotinic receptor-ligand interactions with infrared difference spectroscopy. *J. Biol. Chem.* 277:10420–10426.

29. Herz, J. M., D. A. Johnson, and P. Taylor. 1987. Interaction of noncompetitive inhibitors with the acetylcholine receptor. The site specificity and spectroscopic properties of ethidium binding. *J. Biol. Chem.* 262:7238–7247.

30. Sanchez-Ruiz, J. M., and M. Martinez-Carrion. 1988. A Fourier-transform infrared spectroscopic study of the phosphoserine residues in hen egg phosvitin and ovalbumin. *Biochemistry.* 27:3338–3342.

31. Shimanouchi, T., M. Tsuboi, and Y. Kyogoku. 1964. Infrared spectra of nucleic acids and related compounds. *Adv. Chem. Phys.* 8:435–498.

32. Hübner, W., and H. H. Mantsch. 1991. Orientation of specifically 13C=O labeled phosphatidylcholine multilayers from polarized attenuated total reflection FT-IR spectroscopy. *Biophys. J.* 59:1261–1272.

33. Mantsch, H. H., A. Martin, and D. G. Cameron. 1981. Characterization by infrared spectroscopy of the bilayer to nonbilayer phase transition of phosphatidylethanolamines. *Biochemistry.* 20:3138–3145.

34. Kooijman, E. E., K. M. Carter, …, B. de Kruijff. 2005. What makes the bioactive lipids phosphatidic acid and lysophosphatidic acid so special? *Biochemistry.* 44:17007–17015.

35. Bell, J. 1985. Protons decrease the single channel conductance of the sarcoplasmic reticulum K^+ channel in neutral and negatively charged bilayers. *Biophys. J.* 48:349–353.

36. Bell, J. E., and C. Miller. 1984. Effects of phospholipid surface charge on ion conduction in the K^+ channel of sarcoplasmic reticulum. *Biophys. J.* 45:279–287.

37. Dickey, A., and R. Faller. 2008. Examining the contributions of lipid shape and headgroup charge on bilayer behavior. *Biophys. J.* 95: 2636–2646.

38. Ellena, J. F., M. A. Blazing, and M. G. McNamee. 1983. Lipid-protein interactions in reconstituted membranes containing acetylcholine receptor. *Biochemistry.* 22:5523–5535.

39. Mantipragada, S. B., L. I. Horváth, …, D. Marsh. 2003. Lipid-protein interactions and effect of local anesthetics in acetylcholine receptor-rich membranes from *Torpedo marmorata* electric organ. *Biochemistry.* 42:9167–9175.

40. Brusés, J. L., N. Chauvet, and U. Rutishauser. 2001. Membrane lipid rafts are necessary for the maintenance of the α7 nicotinic acetylcholine receptor in somatic spines of ciliary neurons. *J. Neurosci.* 21:504–512.

41. Marchand, S., A. Devillers-Thiéry, …, J. Cartaud. 2002. Rapsyn escorts the nicotinic acetylcholine receptor along the exocytic pathway via association with lipid rafts. *J. Neurosci.* 22:8891–8901.

42. Labriola, J. M., C. J. B. daCosta, …, J. E. Baenziger. 2010. Phospholipase C activity affinity purifies with the Torpedo nicotinic acetylcholine receptor. *J. Biol. Chem.* Feb 4. [Epub ahead of print].